Global Change Biology
celebrating 20 years

Global Change Biology (2015) **21**, 431–444, doi: 10.1111/gcb.12672

Carbon accumulation of tropical peatlands over millennia: a modeling approach

SOFYAN KURNIANTO[1,2†], MATTHEW WARREN[3], JULIE TALBOT[1,4], BOONE KAUFFMAN[5], DANIEL MURDIYARSO[2,6] and STEVE FROLKING[1]

[1]*Institute for the Study of Earth, Oceans and Space and Department of Earth Sciences, University of New Hampshire, Morse Hall 8, College Road, Durham, NH 03824, USA,* [2]*Center for International Forestry Research, Jalan CIFOR, Situ Gede, Bogor 16115, Indonesia,* [3]*USDA Forest Service, Northern Research Station, Durham, NH 03824, USA,* [4]*Department of Geography, Université de Montréal, C.P. 6128 Succursale Centre-ville, Montréal, QC H3C 3J7, Canada,* [5]*Department of Fisheries and Wildlife, Oregon State University, Corvallis, OR 97331, USA,* [6]*Department of Geophysics and Meteorology, Bogor Agricultural University, Bogor 16115, Indonesia*

Abstract

Tropical peatlands cover an estimated 440 000 km^2 (~10% of global peatland area) and are significant in the global carbon cycle by storing about 40–90 Gt C in peat. Over the past several decades, tropical peatlands have experienced high rates of deforestation and conversion, which is often associated with lowering the water table and peat burning, releasing large amounts of carbon stored in peat to the atmosphere. We present the first model of long-term carbon accumulation in tropical peatlands by modifying the Holocene Peat Model (HPM), which has been successfully applied to northern temperate peatlands. Tropical HPM (HPMTrop) is a one-dimensional, nonlinear, dynamic model with a monthly time step that simulates peat mass remaining in annual peat cohorts over millennia as a balance between monthly vegetation inputs (litter) and monthly decomposition. Key model parameters were based on published data on vegetation characteristics, including net primary production partitioned into leaves, wood, and roots; and initial litter decomposition rates. HPMTrop outputs are generally consistent with field observations from Indonesia. Simulated long-term carbon accumulation rates for 11 000-year-old inland, and 5 000-year-old coastal peatlands were about 0.3 and 0.59 Mg C ha^{-1} yr^{-1}, and the resulting peat carbon stocks at the end of the 11 000-year and 5 000-year simulations were 3300 and 2900 Mg C ha^{-1}, respectively. The simulated carbon loss caused by coastal peat swamp forest conversion into oil palm plantation with periodic burning was 1400 Mg C ha^{-1} over 100 years, which is equivalent to ~2900 years of C accumulation in a hectare of coastal peatlands.

Keywords: carbon sequestration, holocene, land-use change, oil palm, peat carbon stocks, peat swamp forests

Received 2 May 2014 and accepted 3 June 2014

Introduction

Tropical peatlands, covering approximately 440 000 km^2 or ~10% of the global peatland area (Page *et al.*, 2011), have been persistent carbon sinks through the Holocene (from about 11 600 years ago to the present), contributing a significant influence on the global carbon budget (Yu, 2011). Southeast Asia contains about 60% of the tropical peat area, with about 210 000 km^2 in Indonesia, and 26 000 km^2 in Malaysia (Page *et al.*, 2011). Tropical peatlands store about 40–90 Gt C overall, and Southeast Asian peatlands account for 77% of that stock (Yu *et al.*, 2010; Page *et al.*, 2011). Data collected from 26 sites throughout the tropics indicate that the tropical peatlands long-term mean carbon accumulation rate during the Holocene averaged 12.8 g C m^{-2} yr^{-1}, although rates as high as 56.2 g C m^{-2} yr^{-1} are reported from Central Kalimantan, Indonesia (Page *et al.*, 2004; Yu *et al.*, 2010). High rates of organic matter accumulation as peat are generated by high productivity of tropical peat swamp forests (PSFs) and low decomposition rates due to soil saturation (Chimner & Ewel, 2004). Low drainage gradients and high precipitation result in soil saturation and anaerobic conditions necessary for tropical peat development, and the acidic, nutrient poor conditions common in ombrotrophic peatlands further impede decomposition (Chimner & Ewel, 2005; Dommain *et al.*, 2011).

In Southeast Asia, inland peat formation began as early as 20–30 thousand calendar years before present (hereafter kBP; Anshari *et al.*, 2004), though most peatlands initiated in the early Holocene, around 11–8 kBP

†Present address: Department of Fisheries and Wildlife, Oregon State University, Corvallis, OR 97331, USA

Correspondence: Steve Frolking, tel. +1 603 862 0244, fax +1 603 862 0188, e-mail: steve.frolking@unh.edu

(Neuzil, 1997; Yu *et al.*, 2010). Coastal peatland development initiated later, around 7 kBP (Dommain *et al.*, 2011), with the youngest peatlands beginning from <2 kBP (Yu *et al.*, 2010). However, the rate of peat accumulation in coastal peatlands has been faster than for inland peatlands, averaging 1.8 and 0.5 mm yr^{-1}, respectively, apparently due to a weaker coastal influence of decreased precipitation and higher ENSO (El Niño Southern Oscillation) intensity over the past several millennia (Dommain *et al.*, 2011). Rieley *et al.* (2008) reported peat accumulation rates in tropical peat swamp ecosystems, especially in Southeast Asia, to vary between 0–3 mm yr^{-1}, with a median value of 1.3 mm yr^{-1}. Using a mean tropical dry peat density of 90 kg m^{-3} and carbon concentration of 0.56 kg C kg^{-1} (Page *et al.*, 2011), this is equivalent to about 70 g C m^{-2} yr^{-1}.

Recently, tropical peat swamp forests have been heavily impacted by increased rates of deforestation and land conversion. During 2000–2010, the upland deforestation rate in Southeast Asia was 1% yr^{-1}, while PSF deforestation was 2.2% yr^{-1} (Miettinen *et al.*, 2011). Tropical PSF deforestation releases carbon to the atmosphere not only from the loss of aboveground biomass (Miettinen & Liew, 2010) but also from enhanced peat decomposition due to the lowering of the water table level (Hooijer *et al.*, 2010), and peat combustion from fire (Page *et al.*, 2002; Heil *et al.*, 2006). PSF conversion into oil palm plantations (a dominant land-use change in the region) results in loss of about 16 Mg C ha^{-1} yr^{-1}, mostly as CO_2 (Hergoualc'h & Verchot, 2011; Koh *et al.*, 2011). This C loss rate from land conversion is about 20 times the mean C uptake rate, and includes emissions from peat burning, changes in aboveground biomass, and peat oxidation (Murdiyarso *et al.*, 2010).

Relative to northern temperate peatlands or upland tropical forests, limited carbon-related field research has been conducted in tropical PSF, thus the influence of climate and land use on tropical PSF carbon are not well understood (Farmer *et al.*, 2011). Ecosystem modeling is one tool that can be utilized to represent and understand dynamic processes in tropical PSFs and, in turn, can be used for assessing the impact of climate change and land-use pressure on peatlands. Several ecosystem models have been developed for simulating carbon dynamics in northern temperate peatlands; however, very few models have been applied for tropical PSF systems (Farmer *et al.*, 2011). Recent work by Mezbahuddin *et al.* (2014) has focused on hourly to seasonal carbon and water dynamics using the detailed, process-based *ecosys* model over 4 years at a drained PSF in Central Kalimantan, Indonesia. Consistent with flux tower data from the site (Hirano *et al.*, 2007), *ecosys* modeling showed that the PSF lost substantial C (~100 g C m^{-2} $month^{-1}$) when the water table was deeper than 1 m, due to strong increases in ecosystem respiration and a relatively weak sensitivity in C uptake (photosynthesis) to water table (WT) depth (Mezbahuddin *et al.*, 2014). In this article, we present a new, simple model of long-term tropical PSF carbon cycling, to explore whether limited existing field data of contemporary carbon dynamics (e.g. net primary productivity, litter decomposition) are consistent with long-term carbon accumulation rates inferred from peat core analysis. We modified the Holocene Peat Model (HPM; Frolking *et al.*, 2010) to simulate carbon accumulation in tropical PSF. Using this modified model, we assess impacts of annual and seasonal precipitation variability on carbon accumulation over millennia, and simulate impacts of land-cover change from pristine forests to oil palm plantations on peatland carbon dynamics.

Materials and methods

Overview of HPMTrop

The Holocene Peat Model is a one-dimensional and annual time step model for estimating the carbon cycle in northern temperate peatlands that has been applied to field studies (Frolking *et al.*, 2010; Tuittila *et al.*, 2012; Quillet *et al.*, 2014) and qualitative analysis (Turetsky *et al.*, 2012). The model integrates a peat decomposition model (Frolking *et al.*, 2001) and dynamic peat accumulation model that couples carbon and water balances (Hilbert *et al.*, 2000). Holocene peat model estimates characteristics of the vegetation and peat column such as litter production, litter decomposition, peat accumulation, hydrological properties of peat, and water table depth.

To apply HPM to tropical peatlands, we developed a new version: HPMTrop, which uses the basic functionalities of HPM to calculate long-term (millennial) carbon dynamics, but with three fundamental changes – plant functional types (PFTs), monthly time step, and water balance calculation – along with some modified parameter values. HPM's northern temperate peatlands PFTs include mosses, sedges, herbs, and shrubs. However, primary production in intact tropical PSF is dominated by trees, while contributions from mosses and other PFTs are negligible (Phillips, 1998). Hence, HPMTrop considers only a tree PFT, with tree net primary productivity (NPP) partitioned into three components (leaves, wood, and roots) that are tracked separately. Tropical climates are warm year-round, with precipitation patterns that can be partitioned into rainy and dry seasons if not uniform throughout the year. To capture the impact of the precipitation seasonality on tropical peat development, HPM was modified from an annual time step to a monthly time step. Tropical PSF water balance models are site-specific and not well developed for general application, (e.g. Susilo *et al.*, 2013; Mezbahuddin *et al.*, 2014) and because few data exist for run-on, runoff, or water table depth in tropical PSF, HPMTrop does not calculate a monthly water balance. Instead HPMTrop uses an empirical

relationship between WT and monthly water deficit to set the monthly WT for NPP and decomposition calculations.

Model Structure

Vegetation. For each month of the simulation, HPMTrop uses the monthly WT to calculate NPP (litter production), peat profile water content, decomposition, and peat depth. Following a relationship between water table depth and gross primary productivity (GPP) measured by eddy covariance in a PSF in Sebangau, Kalimantan (Indonesian Borneo; Hirano *et al*., 2012), we modeled monthly NPP as a quadratic function of water table depth

$$\mathrm{NPP}_j = \mathrm{NPP}_0 \times (-0.3046 \cdot \mathrm{WT}_j^2 + 0.1732 \cdot \mathrm{WT}_j + 0.9874) \quad (1)$$

where NPP_0 is base-level monthly NPP (kg m^{-2} $month^{-1}$, see Table 1), and WT_j is the water depth (m, positive values down from the peat surface) in month j. As in HPM (Frolking *et al*., 2010), PFT biomass is not simulated as a dynamic variable. Instead, monthly tree NPP is disaggregated into three components – leaves, wood, and roots – and added as monthly litterfall to the surface litter layer (leaves and wood) or the uppermost portion of the peat profile (roots are added to the surface peat, down to a maximum rooting depth equal to the larger of 50 cm and the water table depth) (Table 1). While this will not capture the seasonal dynamics of litterfall (which are not well described for tropical PSF), subannual variation is not likely a key factor in long-term peat accumulation. In HPMTrop, the surface litter accumulates and decomposes for 12 months, and then the remaining litter becomes the surface peat cohort at the end of the year, as a layer above the previous year's peat cohort.

Decomposition, peat mass balance, and peat bulk density. HPMTrop peat decomposition follows HPM (Frolking

Table 1 Parameter values used in HPMTrop

Parameter	Description	Value	Units	References
Monthly NPP				
leaves	Monthly leaf production/litterfall	0.079	kg m^{-2} $month^{-1}$	Hergoualc'h & Verchot (2011)
wood	Monthly wood production/litterfall	0.057	kg m^{-2} $month^{-1}$	Chimner & Ewel (2005)
roots	Monthly root production/litterfall	0.025	kg m^{-2} $month^{-1}$	Hergoualc'h & Verchot (2011)
k_0 (initial litter decomposition rate)				
leaves	Initial leaf decomposition mass loss rate	0.1055	$Month^{-1}$	Brady (1997); Chimner & Ewel (2005); Shimamura & Momose (2005); Yule & Gomez (2008)
wood	Initial wood decomposition mass loss rate	0.0224	$Month^{-1}$	Chimner & Ewel (2005)
roots	Initial root decomposition mass loss rate	0.0685	$Month^{-1}$	Chimner & Ewel (2005)
Anoxia scale length				
Coastal	e-folding length for anoxia below WT	0.23	m	
Inland	e-folding length for anoxia below WT	0.30	m	
Root depth (min)		0.5	m	
Peat water content parameters				
W_{min}	Minimum peat pore water content	0.03	m^3 m^{-3}	Frolking *et al*. (2010)
c_1	Peat water content parameter	0.5	—	Frolking *et al*. (2010)
c_2	Peat water content parameter	20	kg m^{-3}	Frolking *et al*. (2010)
Saturation factor for the decomposition rate				
W_{opt}	Peat pore water content for optimum decomposition	0.45	m^3 m^{-3}	Frolking *et al*. (2010)
W_{sat}	Peat pore water content at saturation	1	m^3 m^{-3}	Frolking *et al*. (2010)
f_{max}	Maximum decomposition rate multiplier	1	—	Frolking *et al*. (2010)
f_{sat}	Saturation decomposition rate multiplier	0.3	—	Frolking *et al*. (2010)
f_{min}	Minimum decomposition rate multiplier	0.001	—	Frolking *et al*. (2010)
Bulk density function parameters				
c_5	Bulk density function parameter	0.2	—	Frolking *et al*. (2010)
c_6	Bulk density function parameter	0.1	—	Frolking *et al*. (2010)
ρ_{min}	Minimum peat bulk density	90	kg m^{-3}	Warren *et al*. (2012)
$\Delta\rho$	Maximum increase in bulk density	40	kg m^{-3}	Warren *et al*. (2012)

et al., 2010), however with a monthly time step, and PSF tissue decomposition parameters are based on several studies (e.g. Brady, 1997; Chimner & Ewel, 2005; Shimamura & Momose, 2005; Yule & Gomez, 2008; Table 1). Leaves, wood, and root litter/peat decompose independently in each annual peat cohort (and the surface litter layer). Decomposition rates, k, decline linearly from their initial value, k_0, as the cohort loses mass, $k = k_0(m/m_0)$ (Clymo *et al.*, 1998; Frolking *et al.*, 2001). There is a water content rate multiplier for cohorts above the water table and a different rate multiplier for cohorts below the water table (Frolking *et al.*, 2010). Above the water table, the degree of saturation of a peat cohort (W_l) is determined by two factors: cohort bulk density and cohort distance from the water table, following the formulation in HPM (Frolking *et al.*, 2010). Mass remaining of peat and surface litter cohorts are calculated each month, as the balance of litter input (to the surface litter pool and to the peat cohorts in the root zone) and loss via decomposition. The root input density profile was assumed to be uniform from the surface of the peat down to 0.5 m or the water table depth, whichever depth is greater. Bulk density increases nonlinearly with peat mass loss as in HPM (Frolking *et al.*, 2010), and is computed for each annual cohort. The thickness of each annual peat cohort is calculated as the ratio (cohort mass remaining)/(cohort bulk density). Total peat depth is the sum of all cohort thicknesses. Peat carbon content is set to 0.5 kg C kg^{-1}.

Water table reconstruction. HPMTrop simulates thousands of years of peat accumulation (or loss), and so requires a monthly water table depth reconstruction for the simulation period. We used three steps for generating the water table over the Holocene: (i) developing a linear relationship between monthly water deficit and measured water table, (ii) analyzing 20th century precipitation to generate different monthly precipitation patterns with probabilities related to El Niño, 'normal', and La Niña conditions, and (iii) using proxies to generate long-term (millennial) variability in El Niño probability and total annual precipitation.

Empirical water table model. We used a simple linear regression between estimated monthly PSF water deficit and measured water table to enable us to estimate water table depth driven by long-term monthly precipitation (P_j). Monthly water table depth was measured in Sebangau PSF, Kalimantan, Indonesia, for about 14 years (Wösten *et al.*, 2010). These water table measurements were related to cumulative monthly water deficit, using a common formulation for tropical forests (Hutyra *et al.*, 2005; Aragão *et al.*, 2007; Malhi *et al.*, 2009; Frolking *et al.*, 2011) whereby water deficit, D_j, accumulates in months with $P_j < 100$ mm and diminishes if $P_j > 100$ mm, as

$$D_j = \max[0, D_{j-1} + (100 - P_j)], \quad (2)$$

with D_j and P_j in mm per month. Monthly precipitation was calculated as the spatial average over eight 0.5° grid cells centered on Sebangau (−2.8°S, 113.8°E), from the climate dataset of Matsuura & Willmott (2012). We then calculated a linear relationship between monthly WT depth (in cm) and monthly water deficit (in mm) (Fig. 1)

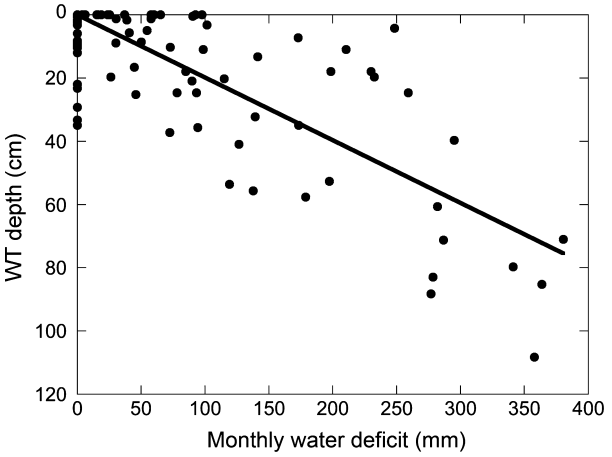

Fig. 1 Relationship between calculated monthly water deficit, D_i [see Eqn (2)], and observed mean monthly water table depth below the peat surface during 1995–2005 (Wösten *et al.*, 2010) at Sebangau, Kalimantan, Indonesia. Linear fit relates D_i in mm to water table depth in cm [see (Eqn 3)].

$$\mathrm{WT}_j = 0.20 D_j \quad (3)$$

Generating stochastic monthly precipitation for El Niño, normal, and La Niña years. El Niño/La Niña dynamics exert a strong control on dry season precipitation in Indonesia (Aldrian & Dwi Susanto, 2003), and this was the basis of our reconstruction. First, 1900–2010 annual precipitation in Sebangau, Kalimantan (Matsuura & Willmott, 2012) was disaggregated into three classes based on each year's southern oscillation index (SOI): El Niño, normal, or La Niña (McKeon *et al.*, 2004), with about half of the years classified as normal years and the remainder divided between El Niño and La Niña. A cluster analysis of monthly precipitation was done for all years in each class – El Niño, normal, and La Niña – using Ward's method for clustering the monthly data based on the dissimilarity matrix calculated using Euclidian distance. The cluster analysis, done with the JMP pro 10 software, resulted in 12 precipitation groups, four in each class. A dendrogram graph showing the precipitation grouping was generated by using dissimilarity distance (Figures S1–S3 in supporting document). The probability of each precipitation group was calculated as the ratio of the number of years within the group generated by cluster analysis to the number of years in its precipitation class. This generated contemporary probabilities for precipitation class (El Niño, normal, and La Niña) and, within class, four different monthly precipitation patterns (Figure S4; Kurnianto, 2013). Predicted monthly precipitation could then be used with the empirical WT model to generate monthly WT values to drive HPMTrop simulations.

Holocene variability in precipitation/water table depth. Precipitation class probabilities and magnitudes through the Holocene were modified from 20th century values based on paleoclimate reconstruction. Reconstructions from the region

indicate that the intensity and frequency of El Niño Southern Oscillation (ENSO) were low early in the Holocene, increased substantially around 4 kBP, and further intensified up to the present (Sandweiss *et al*., 2001; Conroy *et al*., 2008; Cobb *et al*., 2013). In addition, oxygen isotope content ($\delta^{18}O$) sampled from cave stalagmites in northern Borneo indicates wetter conditions around 5 kBP relative to both earlier and later in the Holocene (Partin *et al*., 2007; Griffiths *et al*., 2009).

We modified El Niño probabilities through the Holocene based on the time series of El Niño frequency in 100-year overlapping windows through the Holocene (Moy *et al*., 2002). These data were averaged in 1000-year intervals and probabilities were standardized by using the frequency of El Niño in the 20th century. For each year of the simulation, we randomly chose a precipitation class (El Niño, normal, or La Niña) based on the reconstructed probabilities, then selected one of the four monthly precipitation time series (see Figure S4) for that class, based on the 20th century probabilities. We then scaled the magnitude of annual (and equivalently, monthly) precipitation throughout the Holocene based on the pattern of oxygen isotope content ($\delta^{18}O$) from stalagmite samples from Borneo (Partin *et al*., 2007). Thus, a complete monthly precipitation time series was generated by combining these two long-term trends (El Niño probability and annual precipitation) with the interannual variability based on the ENSO probabilities and monthly precipitation probability in 20th century generated by the cluster analysis. We then used Eqns (2,3) to generate monthly water table depths for the entire simulation. Note that El Niño intensity – represented by the four possible monthly precipitation scenarios and their relative probabilities (see Figure S4) – was not changed over the simulation.

Model Calibration

A simple model calibration between simulated peat age–depth profiles and field data from peat cores in South East Asia, particularly in Sumatra, Borneo, and peninsular Malaysia (Dommain *et al*., 2011), was used to set the values of the anoxia scale length parameter and a water table offset for coastal peatlands. Based on the characteristics of peat development and their distance to the sea, Dommain *et al*. (2011) distinguished peat profiles as coastal (N = 15 cores), inland peatlands (N = 11), and Kutai peatlands (N = 4). The Kutai peatlands were excluded from this study as they are a disjunct peat formation in East Kalimantan, Indonesia and data necessary to calibrate HPMTrop to this type of peatland are not available. We simulated peat profiles for both coastal and inland types by (i) using different anoxia scale length values (Table 1), (ii) adjusting the water table for coastal peatlands 25% closer to the peat surface compared to inland peat, and (iii) using different peat initiation times of 5 and 11 kBP for coastal and inland peatlands, respectively (Dommain *et al*., 2011). Anoxia scale length is a constant model parameter that controls how steeply decomposition rates decline to full anoxia (minimum decomposition rate) with depth below the water table (Frolking *et al*., 2010); i.e. it represents an effective redox gradient. We calibrated the anoxia scale length parameter in the model simulation to generate typical accumulation rates for coastal and inland peatlands, based on the age–depth data of Dommain *et al*. (2011).

Sensitivity analysis

We conducted basic sensitivity simulations, adjusting individual parameters (typically by ±25%; Table 2) using peat depth and peat mass at the end of the simulation as the model response. Parameters adjusted were NPP_0 and k_0 values for plant components (leaves, wood, and roots), anoxia scale length, bulk density parameters, and monthly precipitation. We also simulated different moisture seasonality for a set of coastal PSF scenarios with mean annual WT of 0.1 m.

Land-cover change scenario

HPMTrop was used to assess the impact of PSF conversion into oil palm on carbon dynamics. The assumptions used in this scenario were:

- The palm plantation continues for the final 100 years of the coastal simulation, with a 25-year crop rotation.
- Drainage ditches were installed to lower monthly WT by 60 cm (Melling *et al*., 2005); these drainage ditches were 'maintained' so the lower water table persisted even as the peat surface lowered due to decomposition (net mass loss). While drainage ditches will have a variable impact on the increase in water table depth across a peatland, with decreasing impact laterally away from the ditch (e.g. Verry *et al*., 2011), this is not considered in these simulations, as HPMTrop has only a vertical peat profile.
- At the beginning of each 25-year oil palm rotation, the site was burned, removing the upper 20 cm of peat and all remaining aboveground biomass (Hergoualc'h & Verchot, 2011).
- During oil palm rotations, constant leaf litter (0.025 kg m^{-2} $month^{-1}$) and root input rate (0.06 kg m^{-2} $month^{-1}$) values were used (Hergoualc'h & Verchot, 2011).

Changes in peat volume due to compaction and consolidation following drainage are not included in the model.

Results

Long-term apparent carbon accumulation rates

The simulated apparent peat accumulation rate for any year, which can be compared to accumulation rates measured in peat cores, is equal to annual peat cohort thickness at the end of simulation (as if the simulated peat were 'cored' at 0 kBP). For coastal peatlands, the simulated peat accumulation rate was initially about 1.1 mm yr^{-1} and dropped quickly to about 0.9 mm yr^{-1} at 3.5 kBP, then increased to about 1.1 mm yr^{-1} at 2.2 kBP (Fig. 2). In recent years, the apparent peat accumulation increased to ~1.6 mm yr^{-1} due to recent peat cohorts being less fully decomposed

Table 2 Sensitivity analysis for the coastal peatland scenario. Peat carbon mass remaining for each tree litter component, total peat carbon, peat depth, total NPP (Mg C ha^{-1}) through the 5000 year simulation, and C/NPP (mass of carbon in peat at the end of the simulation compared to total NPP input, as a percentage) were chosen as the model responses. Base run values are the model output simulated using the default parameters shown in Table 1. Parameters were adjusted ± 25%

				Peat carbon (Mg C ha^{-1})						
No	Parameter		Value	leaves	wood	roots	C (total)	Depth (m)	total NPP	C/NPP (%)
1	base run			480	1810	920	3210	6.0	47900	6.7
2	NPP	Leaves	0.099	667	2000	976	3640	6.8	53700	6.8
3			0.059	311	1580	848	2740	5.1	42000	6.5
4		Wood	0.071	635	2930	1090	4650	8.7	52100	8.9
5			0.043	327	937	725	1990	3.7	43600	4.6
6		Roots	0.031	507	1900	1220	3620	6.7	49700	7.3
7			0.019	455	1720	650	2820	5.2	46000	6.1
8		total	0.246	916	3320	1490	5720	10.7	59800	9.6
9			0.147	192	736	444	1370	2.5	35900	3.8
10	k	Leaves	0.132	326	1620	860	2810	5.2	47900	5.9
11			0.079	770	2050	994	3810	7.1	47900	8.0
12		Wood	0.028	393	1200	807	2400	4.4	47900	5.0
13			0.017	610	2920	1090	4620	8.6	47900	9.6
14		Roots	0.086	457	1730	720	2910	5.4	47900	6.1
15			0.051	488	1840	1200	3530	6.6	47900	7.4
16		total	0.246	244	992	570	1810	3.3	47900	3.8
17			0.147	976	3270	1470	5720	10.8	47900	12.0
18	anoxia scale length		0.29	340	1300	551	2190	4.1	47900	4.6
19			0.17	681	2490	1420	4590	8.6	47900	9.6
20	minBD		112.5	313	1210	689	2210	3.4	47900	4.6
21			67.5	749	2710	1210	4670	11.1	47900	9.8
22	deltaBD		50	447	1690	875	3020	5.4	47900	6.3
23			30	504	1900	953	3350	6.5	47900	7.0
24	BD_c1		0.25	489	1840	926	3260	6.1	47900	6.8
25			0.15	468	1770	915	3150	5.8	47900	6.6
26	BD_c2		0.125	466	1760	906	3140	5.8	47900	6.6
27			0.075	504	1890	949	3340	6.3	47900	7.0
33	P multiplier		1.25	572	2130	1030	3730	6.9	47900	7.8
34			0.75	307	1180	660	2150	4.0	47900	4.5
35	WT multiplier		1.25	417	1590	805	2810	5.2	47900	5.9
36			0.75	551	2060	1020	3620	6.8	47900	7.6

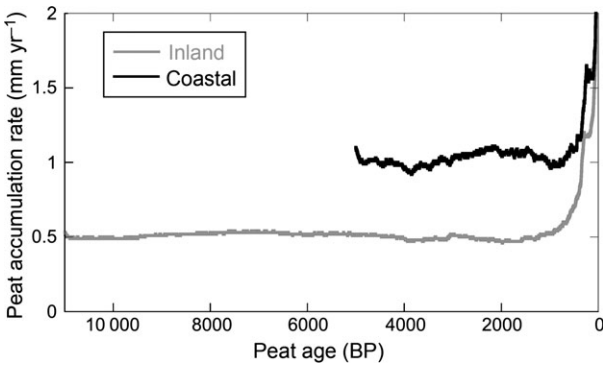

Fig. 2 Simulated peat accumulation rate (mm yr^{-1}) for both coastal and inland peatlands. High apparent accumulation rates for the youngest peat cohorts (less than a few hundred years old) are artifacts reflecting the incomplete decomposition of young, surface peat.

than older, deeper cohorts. Overall, the long-term carbon accumulation rate in the coastal peatlands, calculated as the average yearly cohort thickness is 1.1 mm yr^{-1} or ~0.59 Mg C ha^{-1} yr^{-1} and it yields a total carbon accumulation of about 2900 Mg C ha^{-1} at the end of the 5000-year simulation (Fig. 3).

Over an 11000-year simulation, the inland peatlands had a lower peat accumulation rate compared to coastal peatlands, ranging from 0.4 to 1.4 mm yr^{-1} (Fig. 2) with a simulated long-term apparent peat accumulation rate of 0.5 mm yr^{-1} (0.3 Mg C ha^{-1} yr^{-1}). The simulated carbon storage in inland peat that accumulates over 11 000 years is about 3300 Mg C ha^{-1} (Fig. 3).

The high apparent accumulation rates for the youngest peat cohorts, less than a few hundred years old (Fig. 2), reflect the incomplete decomposition of the young, surface peat. This generates a slightly steeper

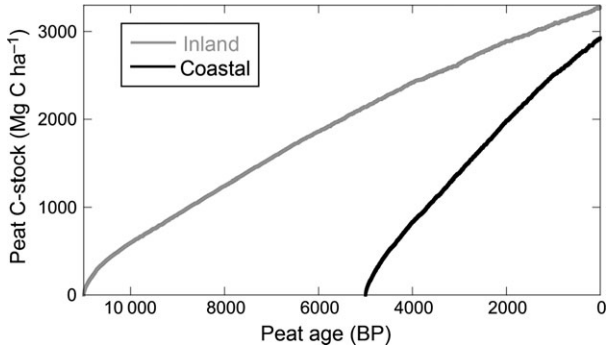

Fig. 3 Simulated accumulating peat carbon stocks (Mg C ha^{-1}) for both inland and coastal peatlands.

simulated age–depth profile near the surface (Fig. 4). Aside from this young-peat artifact, the simulated variability in peat accumulation rate in inland peatlands over 11 000 years was generally low (Fig. 2), resulting in a slow decline in overall peat mass accumulation rate (Fig. 3) and a relatively linear age–depth profile that reaches a depth of 6.0 m (Fig. 4). The coastal PSF simulation had higher variability in peat accumulation rate than the inland peatlands (Fig. 2), but again this did not lead to significant curvature in the age-C mass profile (Fig. 3). Over 5000 years, there was a relatively linear relationship between peat age and depth, and a maximum depth of about 5.4 m (Fig. 4). The simulated decay rate of the deep peat was about 7×10^{-5} yr^{-1}.

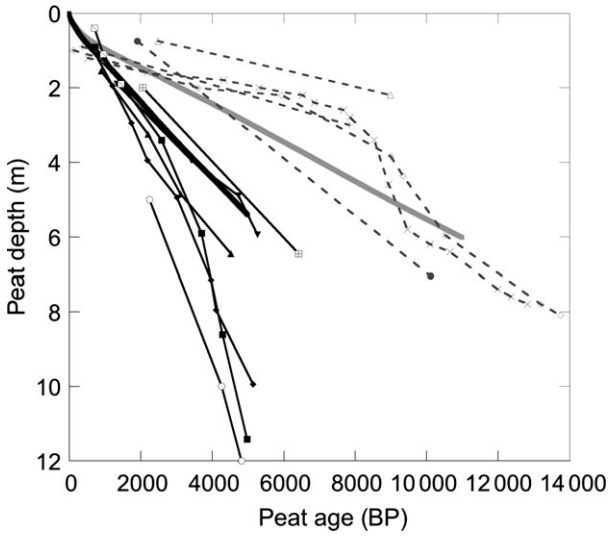

Fig. 4 Simulated peat age–depth profile at the end of the simulations (heavy solid lines) for the inland (gray) and coastal (black) peatlands, overlaid with measured age–depth profiles of coastal (solid lines) and inland (dashed lines) peatlands from Southeast Asia. Measured peat depth–age profiles were obtained from Dommain *et al.* (2011).

Sensitivity analysis

Sensitivity runs were done for the coastal PSF (Table 2). Increasing total tree litter production (leaves, wood, and roots) by 25%, while leaving the decomposition parameters and water table depths unchanged, increased the peat carbon after 5000 years by about 80% and, hence, increased the final peat depth to 10.7 m at the end of simulation. The fraction of total NPP remaining as peat carbon at the end of the simulation increased by about 40% from 6.7% in the base run to 9.6%, so the final peat storage increase both in absolute magnitude and as a fraction of NPP, with about 20% of the additional NPP stored as peat due to more rapid burial in the permanently saturated zone. Conversely, decreasing the total tree productivity by 25% reduced the peat mass remaining by about 60%, and the peat depth by about 60%.

Litter quality, represented by k_0, is the main factor of the decomposition component of the mass balance equation. Increasing the k_0 for all three tree components by 25% reduced the coastal PSF peat accumulation at the end of the simulation by ~45%, due to the higher decomposition rate, and hence reduced the final peat depth 45%. Total NPP was the same in all k_0-sensitivity simulations as it was only influenced by the water table. Therefore, the fraction of the total NPP that remains as peat, *C/NPP*, reduced with an increase of k_o. Among three litter components, the model is most sensitive to the change of the k_0 of wood; reducing wood's k_0 to 0.017 month^{-1} (25%) resulted in an increase ~45% of both peat carbon and peat depth.

The anoxia scale length regulates simulated peat accumulation by affecting the decomposition rate of peat cohorts located near to, but below the water table. Increasing the anoxia scale length by 25% reduced the coastal PSF peat carbon, depth, and the ratio of peat carbon to NPP by about 30%. Decreasing the value of anoxia scale length to 0.17 m led to an increase of about 45% in peat carbon, depth, and *C/NPP* after 5000 years.

Sensitivity analyses on the multiplier of the precipitation pattern based on δ^{18}O of cave stalagmites and the linear relationship for estimating water table were also performed. Increasing monthly precipitation by 25% generated an increase in coastal PSF peat mass remaining of ~15%, and also increased the peat depth by the same magnitude, due to unchanged bulk density parameters. Simulating a drier climate over 5000 years by reducing the precipitation multiplier by 25% reduced the peat mass and peat depth about 30%. Increasing the monthly water table depth by 25% resulted in a decrease in peat mass remaining and peat depth by ~15% at the end of the simulation.

Finally, we conducted a set of sensitivity simulations with mean annual water table of 0.1 m, but with different precipitation seasonality, from none (setting the monthly water table to a constant value of 0.1 m) to extreme (1 month with 1.2 m WT and 11 months with 0.0 m WT). Coastal PSF peat C accumulation over 5000 years decreased with increasing precipitation seasonality by about 10% across this range (Fig. 5).

Land-cover change scenario

The simulated coastal PSF accumulated 2870 Mg C ha^{-1} prior to conversion into oil palm, and then rapidly lost nearly half that mass in the 100 years following forest conversion (Fig. 6). The simulated carbon loss of 1370 Mg C ha^{-1} over the period of 100 years generated by land-cover change and current management practices was equivalent to peat accumulation over the previous 2900 years. Put differently, in 1 year it would require an area of about 2300 ha of pristine coastal PSF to sequester the amount of carbon lost over 100 years from just one hectare of converted area. Despite ongoing litter inputs from the oil palm, periodic burning resulted in a truncated peat age–depth profile, with the near-surface peat dating to about 2400 BP after 4 oil palm rotations with burning. At the end of the simulation with four, 25-year rotations of oil palm planting and burning, the peat depth was about 2.6 m, down ~3 m from the simulation run without forest conversion. Burning directly removed 0.8 m of peat (0.2 m per burn in each rotation); about 2 m of peat was lost to oxidation. Aside from direct removal via burning, peat subsidence simulated from HPMTrop was only caused by peat oxidation (i.e. mass loss) and a resulting increase in bulk density with peat humification (though much of the lower density surface peat was burned off every 25 years), but neglected any consolidation and compaction components of subsidence that arise directly from dewatering the peat, which can be particularly significant in the initial few years after drainage (e.g. Couwenberg *et al.*, 2009; Hooijer *et al.*, 2010; Jauhiainen *et al.*, 2012).

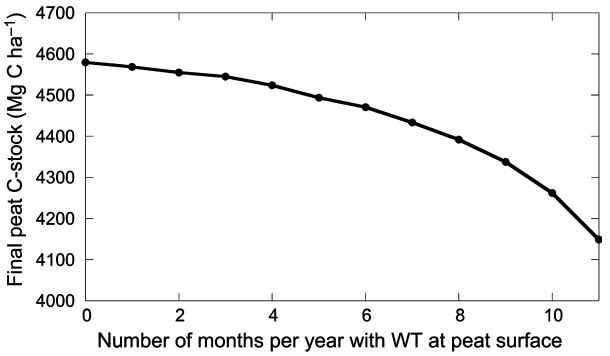

Fig. 5 Variation in coastal peat swamp forests (PSF) peat C accumulation (final C stock after 5000 years) for scenarios with constant mean annual WT depth of 0.1 m, but with different wetness seasonalities. The *X*-axis is number of months per year with the water table at the peat surface (WT = 0 m). For example, 0 is 12 months with WT = 0.1 m and 0 months with WT = 0 m; 6 is 6 months with WT = 0.2 m and 6 months with WT = 0 m, 9 is 3 months with WT = 0.4 m and 9 months with WT = 0 m, and 11 is 1 month with WT = 1.2 m and 11 months with WT = 0 m.

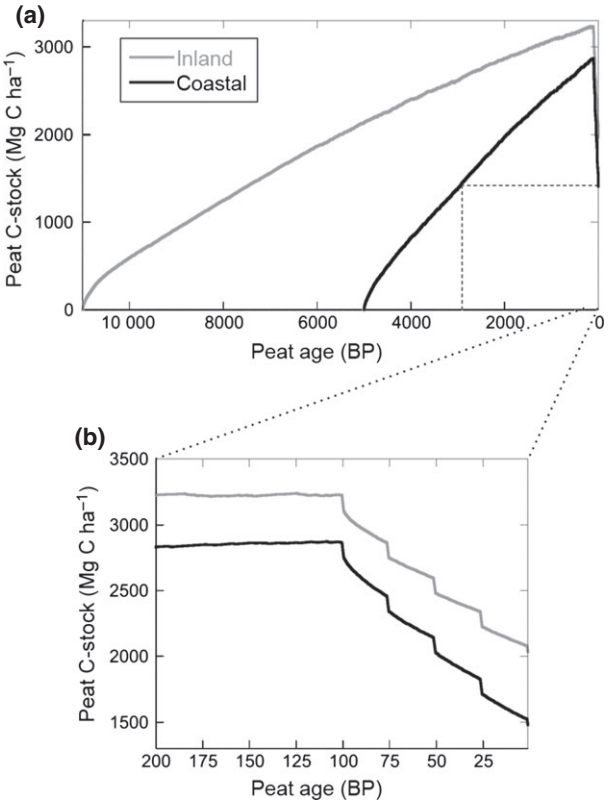

Fig. 6 (a) Simulated peat mass accumulation for coastal peatlands over 5000 years and inland peatland over 11 000 years, with conversion into oil palm (forest cleared and peat drained) and periodic burning (every 25 years) during the last 100 years of the simulation. Land-use conversion causes coastal peatland to lose about 3000 years of peat accumulation (dashed lines). (b) Zoom in on final 200 years of the simulations; vertical drops in peat mass are a result of burning off 20 cm of peat every 25 years.

For the simulated inland PSF, accumulated peat mass reached about 3240 Mg C ha^{-1} before forest conversion and reduced to 2080 Mg C ha^{-1} due to oil palm conversion (Fig. 6). The carbon loss resulting from that scenario was about 1 160 Mg C ha^{-1} over 100 years (~12 Mg C ha^{-1} yr^{-1}; averaging over episodic burning); it required about 5500 years to accumulate the final 1160

Mg C ha^{-1}. The peat depth at the end simulation was 3.6 m, down about 2.4 m from the pristine scenario (again with 0.8 m lost directly to burning), generating a truncated peat age–depth profile. For the inland scenario, annual C sequestration from 3900 ha of pristine Southeast Asian PSF would be required to offset the C lost from 100 years cultivation of a single hectare.

Discussion

HPMTrop is the first process-based model to simulate long-term (decadal to millennial) carbon accumulation dynamics in tropical peat ecosystems. Using a simple carbon balance as the difference between tree productivity and decomposition rates, and including the effects on decomposition rates of a water table that varies seasonally and interannually, HPMTrop simulates (i) annual peat cohort mass and thickness and (ii) total peat profile carbon stocks and peat depth.

Carbon accumulation rates in tropical PSF during the Holocene

There were two dominate regional changes during the late Pleistocene and Holocene that influenced the regional hydrology of Indonesian peatlands – changes in sea level and changes in precipitation. The abrupt rise in sea level in the early Holocene led to inundation of the Sunda Shelf, which had been exposed during the last glacial maximum (Smith *et al*., 2011) and, hence, increased the regional evaporating area as a source of moisture. This, coupled with an increase in sea surface temperature (SST) in the western equatorial Pacific (Rosenthal, 2003), may have increased convective forcing, resulting in higher precipitation in Southeast Asia. Although sea-level rise would also have affected the rate of continental runoff, and thus perhaps inundation depths and duration in flat coastal plains (Dommain *et al*., 2011), we did not consider this in the HPMTrop simulations reported here.

During the Holocene, Southeast Asian precipitation varied, influenced by multiple factors: northern summer insolation, mean position of Intertropical Convergence Zone (ITCZ), sea surface temperature, and sea-level rise (Wang *et al*., 2005; Griffiths *et al*., 2009). Precipitation reconstruction based on $\delta^{18}O$ speleothems sampled from cave stalagmite calcite in northern Borneo (Partin *et al*., 2007) and Liang Luar, Flores, Indonesia (Griffiths *et al*., 2009), demonstrated that annual precipitation in the mid-Holocene was higher than in both the late Pleistocene/early Holocene and the present. However, the two paleo-reconstructions show different patterns: stalagmite $\delta^{18}O$ from northern Borneo indicate a precipitation maximum occurred ~4 kBP; while at Liang Luar it was ~7 kBP. In addition, El Niño began to intensify about 6 kBP (Sandweiss *et al*., 2001; Conroy *et al*., 2008; Cobb *et al*., 2013), which probably caused a decrease in precipitation, at least in some years, in the Indonesian region (Aldrian & Dwi Susanto, 2003).

In the early Holocene, 11–10 kBP, inland peatlands were in early phases of development, possibly caused by sea-level rise on the Sunda Shelf associated with the last deglaciation (Steinke *et al*., 2003; Dommain *et al*., 2011). HPMTrop simulated an initial peat accumulation rate for inland peatlands of about 0.49 mm yr^{-1} (~0.26 Mg C ha^{-1} yr^{-1}). This value is slightly lower than published peat accumulation rates ranging between 0.6 and 0.8 mm yr^{-1} recorded from inland peatland cores collected in the Sebangau catchment, Kalimantan, dated from 13 to 10 kBP, and the Palangkaraya peatlands dated at 9 kBP (Neuzil, 1997; Page *et al*., 2004). C accumulation rates recorded from a core sampled in the Sebangau catchment ranged from 0.18 to 0.33 Mg C ha^{-1} yr^{-1} (Page *et al*., 2004) which is lower than 0.5 to 0.7 Mg C ha^{-1} yr^{-1} measured from adjacent peatlands in Palangkaraya, Kalimantan (Neuzil, 1997). Around 8 to 7 kBP, simulated peat accumulation rates for the inland peatland scenario were about 0.5 mm yr^{-1}, equivalent to a carbon accumulation rate of 0.29 Mg C ha^{-1} yr^{-1}. This value is consistent with accumulation rates for the same time period measured from a peat core sampled in the Sebangau catchment, which ranged from 0.4 to 0.9 mm yr^{-1} (0.2 to 0.5 Mg C ha^{-1} yr^{-1}), however higher values were observed in a core from the Palangkaraya peatlands where the accumulation rate was 1.2 mm yr^{-1} (Neuzil, 1997).

From 6 to 5 kBP, the mean peat accumulation rate in Sebangau was 0.23 mm yr^{-1}, with an average carbon accumulation rate of 0.1 Mg C ha^{-1} yr^{-1} (Page *et al*., 2004). Based on peat cores sampled from an inland peatland in Kalimantan, peat accumulation rates were reduced from ~0.8 mm yr^{-1} circa 8 kBP to about 0.5 mm yr^{-1} around 5 kBP (Dommain *et al*., 2011). Simulated rates were consistent with this trend, with a peat accumulation rate of 0.51 mm yr^{-1} at 5 kBP, which is equivalent to carbon accumulation of 0.28 Mg C ha^{-1} yr^{-1}.

In coastal Sumatra and Kalimantan, however, peat initiation began at higher accumulation rates in the period after 7 kBP. A core taken from Bengkalis Island, near Sumatra shows that the onset of peatland development in this area was 5.8 kBP, with an initial accumulation rate of about 2.5 mm yr^{-1} and carbon accumulation of about 5.7 Mg C ha^{-1} yr^{-1} (Neuzil, 1997). Dommain *et al.* (2011) also reported that the accumulation rate during the initial development of coastal peatlands in Sumatra, peninsular Malaysia, and

Borneo was about 1.7 mm yr^{-1} at 6 to 5 kBP. HPMTrop simulated rates for the coastal peatlands scenario were lower, with about 1.0 mm yr^{-1} of peat accumulation in the early stage of development (~5 kBP).

After 5 kBP, sea level gradually decreased from 5 m above present mean sea level (MSL) to the present MSL (Steinke *et al.*, 2003). Decreasing precipitation in the western part of Indonesia was probably associated with the weakening of both the East Asian summer monsoon (Wang *et al.*, 2005) and the Australian-Indonesian summer monsoon (Griffiths *et al.*, 2009) as well as more frequent El Niño (Cobb *et al.*, 2013). Slowly declining sea level, combined with decreasing precipitation, led to a decline in the water table and enhanced organic matter decomposition, and thus a lower peat accumulation rate. From ~5 kBP onward, declines in HMPTrop-simulated peat accumulation rates were minimal in both inland and coastal peatlands; HPMTrop would respond to changes in precipitation only, as the impact of sea-level decline on continental runoff and groundwater levels was not incorporated into HPMTrop. Peat accumulation rates were 0.46 mm yr^{-1} (0.25 Mg C ha^{-1} yr^{-1}) and 1 mm yr^{-1} (0.54 Mg C ha yr^{-1}) in inland and coastal peatlands, respectively. A variable but probably slightly decreasing pattern of accumulation rate was measured from peat cores taken in Southeast Asia, with mean values ~0.3 mm yr^{-1} for inland peatlands and ~1.5 mm yr^{-1} for coastal peatlands (Dommain *et al.*, 2011).

Impact of land-cover change on PSF carbon dynamics

Tropical PSF are now experiencing strong land-use pressure, including conversion into agriculture or plantation forestry (Koh *et al.*, 2011; Miettinen *et al.*, 2012), which usually includes canal development for lowering the water table (Hooijer *et al.*, 2010) and results in more common peat fires (Page *et al.*, 2002; Saharjo & Munoz, 2005). Both drainage and fires release peat carbon to the atmosphere, and emission factors and process models are needed to inform the development of REDD+ mechanisms (e.g. Murdiyarso *et al.*, 2010) by estimating some of the carbon losses that contribute to the total emissions from land-cover changes occurring on tropical peatlands. In coastal peatlands, the simulation of a 100-year conversion with periodic peat burning reduced the peat carbon by about 1400 Mg C ha^{-1} or ~14 Mg C ha^{-1} yr^{-1} carbon emission due to both peat oxidation and fires (Table 3). The mean annual carbon loss is equivalent to about 30 years of peat accumulation. For inland peatlands, a net carbon loss of ~12 Mg C ha^{-1} yr^{-1} was estimated for the same land-cover change scenario (Fig 6). These carbon loss estimations are conservative values as we did not include the loss from aboveground biomass (e.g. Hergoualc'h & Verchot, 2011). A similar rate of carbon loss of about 10.8 Mg C ha^{-1} yr^{-1} was estimated using a flux change method proposed by IPCC (Hergoualc'h & Verchot, 2011). Based on several years of eddy flux tower data, Hirano *et al.* (2012) reported a ~3 Mg C ha^{-1} yr^{-1} increase in CO_2 emissions in a disturbed and burned site (fern and sedge vegetation, with no remaining trees) compared to a secondary PSF (secondary forest) in Central Kalimantan, Indonesia.

Forest conversion into agriculture, including oil palm plantations, frequently involves burning for land preparation (Saharjo & Munoz, 2005). HPMTrop results showed that total peat carbon at the end simulation following forest conversion without burning is about 2000

Table 3 Reported area and depth of peat burned for combined coastal and inland peatlands in Indonesia, followed by model simulations of carbon stocks and losses from coastal peatlands as a result of land-cover change (LC) and fire (assuming one land clearing fire every 25 years and 20 cm of peat consumed per fire)

Area of peat burnt (ha)	1 450 000	Page *et al.*, 2002
	2 441 000	
	6 804 688	
	1 909 200	Heil *et al.*, 2006
	2 300 500	
	1 331 367	Ballhorn *et al.*, 2009
Thickness of peat burnt (cm)	51 ± 5	Page *et al.*, 2002
	33 ± 18	Heil *et al.*, 2006
	20	Hergoualc'h & Verchot, 2011
Carbon stock at end of simulation (Mg C ha^{-1})		
No LC*	2900	This study
LC only†	2000	This study
LC + fire (20 cm)‡	1500	This study
Carbon loss (Mg C ha^{-1})		
LC only§	−900	This study
LC + fire (20 cm)**	−1400	This study
Carbon loss due to fire (Mg C ha^{-1})††	−125	This study
Total carbon loss (Gt C)§§		
Lower estimate	−0.22	This study
Upper estimate	−1.02	This study

*Simulation without land-cover change.
†Land-cover change simulation – 100 years of drainage, but without peat burning.
‡Land-cover change and peat burning simulation with 20 cm of peat burnt every 25 years.
§Calculated as carbon stock of LC only (2) minus no LC (1).
**Calculated as carbon stock of LC + fire (3) minus no LC (1).
††Calculated as carbon loss of LC + fire (5) – LC only (4) divided by the number of fire occurrences–four in this study.
§§Product of carbon loss due to fire (6) and minimum and maximum areas of peat burnt.

Mg C ha^{-1}. The estimated total carbon stock before conversion is 2900 Mg C ha^{-1}, therefore carbon loss from heterotrophic oxidation is 900 Mg C ha^{-1} over 100 years, equivalent to a rate of 9 Mg C ha^{-1} yr^{-1}. The total carbon loss from simulated forest conversion with burning was 1400 Mg C ha^{-1}, assuming 20 cm of peat is consumed by fire every 25 years. Over 4 rotations (100 years), the simulated peat loss from burning releases about 500 Mg C ha^{-1}, equivalent to 125 Mg C ha^{-1} for each fire. A much higher carbon loss per unit area of 250–320 Mg C ha^{-1} was estimated from the severe 1997 peat fires in the Mega Rice Project, West Kalimantan due to deeper peat burning of 51 ± 5 cm (Page *et al*., 2002). Using the reported range in peat burned area in Indonesia estimated for two different fire seasons, (Table 3), peat burning to 20 cm would release carbon in the range of 0.22 – 1.02 Gt C per fire season.

Our simulation results show that land conversion with burning led to 2.4–2.8 m reductions in peat depth over 100 years, at a fairly constant rate, from 5.4 m to 2.6 m in coastal peatlands and 6.0 m to 3.6 m in inland peatlands; equivalent to mean peat decomposition loss rates of 24 and 28 mm yr^{-1} for inland and coastal, respectively. Measured peat subsidence rates in oil palm were 54 ± 11 mm yr^{-1} when burning was used for land clearing, and about 50 ± 22 mm yr^{-1} in *Acacia* plantations in Sumatra without burning activities (Hooijer *et al*., 2012). These measured values, however, are total subsidence rates, comprising several components: burning (oil palm case), oxidation, compaction (due to heavy machinery and to shrinkage in the aerated zone with drying), and consolidation (of the saturated peat due to changes in overlying buoyancy); oxidation is the dominant component (75% to 90% of total subsidence), although compaction and consolidation dominate the subsidence in the initial few years (Hooijer *et al*., 2012). Similar research from peninsular Malaysia reported an average subsidence rate of 20 mm yr^{-1}, of which 60% was due to peat oxidation and the remaining portion caused by shrinkage (Wösten *et al*., 1997). In the HPMTrop simulations, the subsidence rates were generated by direct burning losses and peat oxidation (plus any resulting increases in bulk density), but with no compaction or consolidation due to dewatering, and were generally about 50–100% of reported total subsidence rates.

Model uncertainty

Tropical PSFs are relatively poorly understood ecosystems, with limited data on various carbon and water cycle processes, and no sites (yet) with comprehensive ecosystem-scale continuous measurements of the different components of carbon balance, as exist for northern peatlands (e.g. Roulet *et al*., 2007; Nilsson *et al*., 2008). On developing a first model to simulate long-term peat accumulation in tropical PSF, HPMTrop was designed to capture each of the fundamental processes – carbon (peat mass) gain through vegetation litter inputs, carbon loss through decomposition, and hydrological controls on the rates of C gain and loss – in a very simple way, thus setting up a framework for improvements as more data become available. This simplicity, coupled with very limited field data, produces several sources of uncertainty inherent to the simulations.

Vegetation NPP and its partitioning into leaf, wood, and root litter fractions (Table 1) come from a limited number of studies (e.g. Chimner & Ewel, 2005; Hergoualc'h & Verchot, 2011). As a result, variation in simulated litter inputs through the Holocene simulations was small. HPMTrop peat accumulation is sensitive to NPP, so improved estimates of PSF NPP and above- and belowground litter production, including their variability in space (e.g. inland vs. coastal peatlands) and time (e.g. El Niño vs. La Niña years), could be used to refine the representation of this process. Long-term observations of tree productivity in PSF are needed to understand the impact of precipitation seasonality on productivity. Similarly, the fundamental decomposition rates come from a single, 12-month litter bag study from Micronesia (Chimner & Ewel, 2005), and it is therefore difficult to even characterize the uncertainty in these parameters, particularly for decomposition over millennia. Note that much of total decomposition occurs in the first few years, and most mass is lost within the first few decades (Moore *et al*., 2005). As the only literature for decomposition rate for wood and roots are from a Micronesian peatlands (Chimner & Ewel, 2005), it is unknown how well this represents conditions and litter qualities in other tropical peatlands, and in particular, PSF in Southeast Asia. Although trees are generally the dominant PFT, other vegetation types are found in tropical PSF, such as herbs, sedges, aroids, pandan, ferns, and epiphytes (Anderson, 1963; Wust & Bustin, 2004).

To accumulate organic matter, decomposition rates must be lower than vegetation productivity; in peatlands this is primarily due to water-logging that creates anoxic conditions. In HPMTrop, the extent of peat saturation was driven by water table position, which is a result of the hydrological interactions of climate conditions, local topography, and peat physical properties. A more robust precipitation reconstruction throughout the Holocene, incorporating both frequency and intensity of ENSO as well as long-term variations in total annual precipitation, and precipitation seasonality,

would improve PSF water table simulations. Water table position is modeled as an annual site-level water balance in HPM (Frolking *et al*., 2010). However, due to uncertainty and lack of field data for model development and testing, HPM's water balance equations were not used in HPMTrop, and instead an empirical water table estimation based on a monthly water deficit was implemented. Improved modeling of water balance would allow for feedbacks between dynamic peat properties and water table variation (Belyea & Baird, 2006; Frolking *et al*., 2010). This may be particularly important in drainage simulations, where deeper, highly decomposed peat can have different hydraulic properties than surface peat (e.g. Belyea & Baird, 2006). Improved data on tropical peat hydraulic characteristics, including water retention and hydraulic conductivity are also needed to enhance modeling of water table position (Dommain *et al*., 2010; Rais, 2011). In addition, installation of a network of drainage ditches in a peatland will generate a predictable spatial pattern of impact on the water table (Verry *et al*., 2011), and the impact is likely to vary over time as the peat surface subsides and the ditches degrade or are maintained. The simulation results presented here do not take these factors into account.

HPMTrop did not vary NPP rates between inland and coastal peatland simulations, therefore more rapid accumulation in the coastal peatlands had to arise from slower decomposition. This was accomplished by two modifications – (i) a shallower water table, and (ii) a shorter anoxia scale length in the coastal peatlands. Anoxia scale length is a parameter that controls the exponential decline in the peat decomposition rate with depth below the water table to full anoxia with minimum decomposition rate. Anoxia scale length is a simple representation of several processes that could influence oxygen penetration below the water table – e.g. high frequency water table variability (i.e. submonthly), inputs of oxygenated rainwater, general diffusion, and plant-mediated gas transport. Based on an *in situ* experiment of peat drying-rewetting, lowering the water table generates oxygen penetration into the peat pores and thus the dissolved oxygen may still be detected below, but close to, the water table (Estop-Aragonés *et al*., 2012). In the scenario for simulating peat accumulation in inland and coastal peatlands, the anoxia scale length values are 0.3 and 0.23 m, respectively. Those values were obtained based on sensitivity tuning by comparing the simulated peat age–depth profiles with the measured profiles reported by Dommain *et al*. (2011). As we had only one set of multi-year water table data available (for an inland peatland), the water table depth adjustment for all noninundated months for coastal peatlands was also set by sensitivity tuning, to a value of 25% closer to the peat surface (shallower). Dommain *et al*. (2011) noted that, relative to inland peatlands in Indonesia, coastal peatlands were not strongly influenced by sea-level decline, or reduced precipitation and El Niño activity over the past several millennia. It was also shown in HPMTrop sensitivity analysis that changing the pattern of water table seasonality affects both carbon stocks and peat depth at the end of simulation (Table 2).

HPMTrop simulation results indicated that a large amount of carbon would be lost from tropical PSF converted to agriculture, due to draining, reduced litter inputs, and burning (Table 3). Nevertheless, this amount of carbon release was generated only by peat oxidation due to peat decomposition and burning. Other carbon forms that could be released from peat, such as methane and fluvial dissolved organic carbon, were not modeled in HPMTrop. A recent study in a disturbed Kalimantan peatland showed that total fluvial organic carbon (comprising dissolved organic carbon and particulate organic carbon) flowing out of a drained disturbed PSF ranged from 88 to 100 g C m^{-2} yr^{-1} (0.88 to 1.0 Mg C ha^{-1} yr^{-1}), potentially increasing the peat carbon loss rate by about 20% (Moore *et al*., 2013). Including both methane emissions and fluxes of dissolved organic carbon are important next steps in model improvement for studying the carbon dynamics in tropical peatlands.

Despite uncertainties and the need for improved long-term ecological observations from tropical peatlands, HPMTrop reproduced observed century- to millennial-scale rates of peat carbon accumulation for inland and coastal PSF. In addition, results from the land-use change scenario emphasize the magnitude of carbon emissions associated with tropical peat swamp conversion, and the thousands of years necessary for hydrologically restored and reforested peatlands to regain the carbon lost in years and decades following conversion. HPMTrop provides the first platform for modeling long-term C dynamics in tropical peatlands, and the model can be modified to accommodate refined or additional inputs aimed to assess the impacts of climate, land management, disturbance, and their interactions on landscape scale peatland C dynamics. Provided adequate data for parameterization, the HPMTrop framework could also be used as a foundation for simulating C dynamics for tropical peatlands beyond Southeast Asia.

Acknowledgements

We thank R. Dommain for providing the peat core age–depth profile data, and for helpful comments on the model. We thank R. Birdsey, R. Kolka, S. Neuzil, and three anonymous reviewers

for helpful comments on an earlier draft. This study was supported by a grant from the USDA Forest Service Indonesia Peatlands, Forest and Climate Change Initiative to SF (USDA-2011-67003-30373), a graduate tuition fellowship to SK from the University of New Hampshire, and the Center for International Forestry Research (CIFOR). Additional support from the USAID-funded Sustainable Wetlands Adaptation and Mitigation Program (SWAMP) was jointly implemented by CIFOR, the USFS, and Oregon State University.

References

Aldrian E, Dwi Susanto R (2003) Identification of three dominant rainfall regions within Indonesia and their relationship to sea surface temperature. *International Journal of Climatology*, **23**, 1435–1452.

Anderson J (1963) The flora of the peat swamp forests of Sarawak and Brunei, including a catalogue of all recorded species of flowering plants, ferns and fern allies. *Gardens Bulletin* Singapore, **20**, 131–228.

Anshari G, Kershaw AP, Van Der Kaars S, Jacobsen G (2004) Environmental change and peatland forest dynamics in the Lake Sentarum area, West Kalimantan, Indonesia. *Journal of Quaternary Science*, **19**, 637–655.

Aragão LEOC, Malhi Y, Roman-Cuesta RM, Saatchi S, Anderson LO, Shimabukuro YE (2007) Spatial patterns and fire response of recent Amazonian droughts. *Geophysical Research Letters*, **34**, L07701.

Ballhorn U, Siegert F, Mason M, Limin S (2009) Derivation of burn scar depths and estimation of carbon emissions with LIDAR in Indonesian peatlands. *Proceedings of the National Academy of Sciences of the United States of America*, **106**, 21213–21218.

Belyea LR, Baird AJ (2006) Beyond 'The limit to peat bog growth': cross-scale feedback in peatland development. *Ecological Monographs*, **76**, 299–322.

Brady MA (1997) *Organic Matter Dynamics of Coastal Peat Deposits in Sumatra*. The University of British Columbia, Indonesia.

Chimner RA, Ewel KC (2004) Differences in carbon fluxes between forested and cultivated micronesian tropical peatlands. *Wetlands Ecology and Management*, **12**, 419–427.

Chimner RA, Ewel KC (2005) A tropical freshwater wetland: II. production, decomposition, and peat formation. *Wetlands Ecology and Management*, **13**, 671–684.

Clymo RS, Turunen J, Tolonen K (1998) Carbon accumulation in peatland. *Oikos*, **81**, 368–388.

Cobb KM, Westphal N, Sayani HR *et al*. (2013) Highly variable El Niño-Southern oscillation throughout the holocene. *Science* (New York, N.Y.), **339**, 67–70.

Conroy JL, Overpeck JT, Cole JE, Shanahan TM, Steinitz-Kannan M (2008) Holocene changes in eastern tropical Pacific climate inferred from a Galápagos lake sediment record. *Quaternary Science Reviews*, **27**, 1166–1180.

Couwenberg J, Dommain R, Joosten H (2009) Greenhouse gas fluxes from tropical peatlands in south-east Asia. *Global Change Biology*, **16**, 1715–1732.

Dommain R, Couwenberg J, Joosten H (2010) Hydrological self-regulation of domed peatlands in south-east Asia and consequences for conservation and restoration. *Mires and Peat* Article, **6**, 1–17.

Dommain R, Couwenberg J, Joosten H (2011) Development and carbon sequestration of tropical peat domes in south-east Asia: links to post-glacial sea-level changes and Holocene climate variability. *Quaternary Science Reviews*, **30**, 999–1010.

Estop-Aragonés C, Knorr K-H, Blodau C (2012) Controls on *in situ* oxygen and dissolved inorganic carbon dynamics in peats of a temperate fen. *Journal of Geophysical Research*, **117**, G02002.

Farmer J, Matthews R, Smith JU, Smith P, Singh BK (2011) Assessing existing peatland models for their applicability for modelling greenhouse gas emissions from tropical peat soils. *Current Opinion in Environmental Sustainability*, **3**, 1–11.

Frolking S, Roulet NT, Moore TR, Richard PJH, Lavoie M, Muller SD (2001) Modeling northern peatland decomposition and peat accumulation. *Ecosystems*, **4**, 479–498.

Frolking S, Roulet NT, Tuittila E, Bubier JL, Quillet A, Talbot J, Richard PJH (2010) A new model of Holocene peatland net primary production, decomposition, water balance, and peat accumulation. *Earth System Dynamics*, **1**, 1–21.

Frolking S, Milliman T, Palace M, Wisser D, Lammers R, Fahnestock M (2011) Tropical forest backscatter anomaly evident in SeaWinds scatterometer morning overpass data during 2005 drought in Amazonia. *Remote Sensing of Environment*, **115**, 897–907.

Griffiths M, Drysdale R, Gagan M *et al*. (2009) Increasing Australian-Indonesian monsoon rainfall linked to early Holocene sea-level rise. *Nature Geoscience*, **2**, 4–7.

Heil A, Langmann B, Aldrian E (2006) Indonesian peat and vegetation fire emissions: study on factors influencing large-scale smoke haze pollution using a regional atmospheric chemistry model. *Mitigation and Adaptation Strategies for Global Change*, **12**, 113–133.

Hergoualc'h K, Verchot LV (2011) Stocks and fluxes of carbon associated with land use change in Southeast Asian tropical peatlands: a review. *Global Biogeochemical Cycles*, **25**, GB2001. doi: 10.1029/2009GB003718.

Hilbert DW, Roulet N, Moore T (2000) Modelling and analysis of peatlands as dynamical system. *Journal of Ecology*, **88**, 230–242.

Hirano T, Segah H, Harada T, Limin S, June T, Hirata R, Osaki M (2007) Carbon dioxide balance of a tropical peat swamp forest in Kalimantan, Indonesia. *Global Change Biology*, **13**, 412–425.

Hirano T, Segah H, Kusin K, Limin S, Takahashi H, Osaki M (2012) Effects of disturbances on the carbon balance of tropical peat swamp forests. *Global Change Biology*, **18**, 3410–3422.

Hooijer A, Page S, Canadell JG, Silvius M, Kwadijk J, Wösten H, Jauhiainen J (2010) Current and future CO2 emissions from drained peatlands in Southeast Asia. *Biogeosciences*, **7**, 1505–1514.

Hooijer A, Page S, Jauhiainen J, Lee WA, Lu XX, Idris A, Anshari G (2012) Subsidence and carbon loss in drained tropical peatlands. *Biogeosciences*, **9**, 1053–1071.

Hutyra LR, Munger JW, Nobre CA, Saleska SR, Vieira SA, Wofsy SC (2005) Climatic variability and vegetation vulnerability in Amazônia. *Geophysical Research Letters*, **32**, L24712.

Jauhiainen J, Hooijer A, Page SE (2012) Carbon dioxide emissions from an *Acacia* plantation on peatland in Sumatra, Indonesia. *Biogeosciences*, **9**, 617–630.

Koh LP, Miettinen J, Liew SC, Ghazoul J (2011) Remotely sensed evidence of tropical peatland conversion to oil palm. *Proceedings of the National Academy of Sciences of the United States of America*, **108**, 5127–5132.

Kurnianto S (2013) *Modeling Long-term carbon accumulation of tropical peat swamp forest ecosystems*. University of New Hampshire, Durham, NH.

Malhi Y, Aragao LEOC, Galbraith D *et al*. (2009) Exploring the likelihood and mechanism of a climate-change-induced dieback of the Amazon rainforest. *Proceedings of the National Academy of Sciences of the United States of America*, **106**, 20610–20615.

Matsuura K, Willmott CJ (2012) *Terrestrial Precipitation: 1900–2010 Gridded Monthly Time Series*. v. 3.01; Center for Climatic Research, Department of Geography, University of Delaware, Newark, DE, USA. Available at: http://climate.geog.udel.edu/~climate/html_pages/Global2011/README.GlobalTsP2011.html (accessed 20 March 2013).

McKeon G, Hall W, Henry B, Stone G, Watson I (2004) *Pasture Degradation and Recovery in Australia's Rangelands: Learning from History*. Queensland Department of Natural Resources, Mines and Energy, Indooroopilly, Qld, Australia.

Melling L, Hatano R, Goh KJ (2005) Soil CO2 flux from three ecosystems in tropical peatland of Sarawak, Malaysia. *Tellus B*, **57**, 1–11.

Mezbahuddin M, Grant RF, Hirano T (2014) Modelling effects of seasonal variation in water table depth on net ecosystem CO_2 exchange of a tropical peatland. *Biogeosciences*, **11**, 577–599.

Miettinen J, Liew SC (2010) Degradation and development of peatlands in Peninsular Malaysia and in the islands of Sumatra and Borneo since 1990. *Land Degradation & Development*, **21**, 285–296.

Miettinen J, Shi C, Liew SC (2011) Deforestation rates in insular Southeast Asia between 2000 and 2010. *Global Change Biology*, **17**, 2261–2270.

Miettinen J, Shi C, Liew SC (2012) Two decades of destruction in Southeast Asia's peat swamp forests. *Frontiers in Ecology and the Environment*, **10**, 124–128.

Moore TR, Trofymow JA, Siltanen M, Prescott C, Group CW (2005) Patterns of decomposition and carbon, nitrogen, and phosphorus dynamics of litter in upland forest and peatland sites in central Canada. *Canadian Journal of Forest Research*, **35**, 133–142.

Moore S, Evans CD, Page SE *et al*. (2013) Deep instability of deforested tropical peatlands revealed by fluvial organic carbon fluxes. *Nature*, **493**, 660–663.

Moy C, Seltzer G, Rodbell D, Anderson D (2002) Variability of El Nino/Southern Oscillation activity at millennial timescales during the Holocene epoch. *Nature*, **420**, 162–165.

Murdiyarso D, Hergoualc'h K, Verchot LV (2010) Opportunities for reducing greenhouse gas emissions in tropical peatlands. *Proceedings of the National Academy of Sciences of the United States of America*, **107**, 19655–19660.

Neuzil SG (1997) Onset and rate of peat and carbon accumulation in four domed ombrogenous peat deposits, Indonesia. In: *Biodiversity and sustainability of tropical peatlands - Proceedings of the International Symposium on Tropical Peatlands* (eds Rieley JO, Page S), pp. 55–72. Samara Publishing Limited, Cardigan, Palangkaraya, Indonesia.

Nilsson M, Sagerfors J, Buffam I *et al*. (2008) Contemporary carbon accumulation in a boreal oligotrophic minerogenic mire - a significant sink after accounting for all C-fluxes. *Global Change Biology*, **14**, 2317–2332.

Page SE, Siegert F, Rieley JO, Boehm HV, Jayak A, Limink S (2002) The amount of carbon released from peat and forest fires in Indonesia during 1997. *Nature*, **1999**, 61–65.

Page SE, Wűst RAJ, Weiss D, Rieley JO, Shotyk W, Limin SH (2004) A record of Late Pleistocene and Holocene carbon accumulation and climate change from an equatorial peat bog(Kalimantan, Indonesia): implications for past, present and future carbon dynamics. *Journal of Quaternary Science*, **19**, 625–635.

Page SE, Rieley JO, Banks CJ (2011) Global and regional importance of the tropical peatland carbon pool. *Global Change Biology*, **17**, 798–818.

Partin JW, Cobb KM, Adkins JF, Clark B, Fernandez DP (2007) Millennial-scale trends in west Pacific warm pool hydrology since the Last Glacial Maximum. *Nature*, **449**, 452–455.

Phillips VD (1998) Peatswamp ecology and sustainable development in Borneo. *Biodiversity and Conservation*, **7**, 651–671.

Quillet A, Garneau M, van Vellen S, Frolking S, Eeva-Stiina T (2014) Integration of palaeo-hydrological proxies into a peatland model: a new tool for palaeoecological studies. Ecohydrology, doi: 10.1002/eco.1501.

Rais DS (2011) Peatland hydrology and its role in tropical peatland sustainability. In: *Proceedings of National Symposium on "Integrating Ecohydrological Principles For Good Water Governance,"* pp. 114–140. The APCE/LIPI in cooperation with the Indonesia National Committee for UNESCO (KNIU), Jakarta. 24 March 2011.

Rieley JO, Wust R, Jauhiainen J *et al*. (2008) Tropical peatlands: carbon stores, carbon gas emissions and contribution to climate change processes. In: *Peatlands and climate change* (ed. Strack M), pp. 148–181. International Peat Society, Jyväskylä, Finland.

Rosenthal Y (2003) The amplitude and phasing of climate change during the last deglaciation in the Sulu Sea, western equatorial Pacific. *Geophysical Research Letters*, **30**, 1428.

Roulet NT, Lafleur PM, Richard PJH, Moore TR, Humphreys ER, Bubier J (2007) Contemporary carbon balance and late Holocene carbon accumulation in a northern peatland. *Global Change Biology*, **13**, 397–411.

Saharjo BH, Munoz CP (2005) Controlled burning in peat lands owned by small farmers: a case study in land preparation. *Wetlands Ecology and Management*, **13**, 105–110.

Sandweiss DH, Maasch KA, Burger RL, Richardson JBI, Rollins HB, Clement A (2001) Variation in Holocene El Niño frequencies : climate records and cultural consequences in ancient Peru. *Geological Society of America*, **29**, 603–606.

Shimamura T, Momose K (2005) Organic matter dynamics control plant species coexistence in a tropical peat swamp forest. *Proceedings of Biological sciences/The Royal Society*, **272**, 1503–1510.

Smith DE, Harrison S, Firth CR, Jordan JT (2011) The early Holocene sea level rise. *Quaternary Science Reviews*, **30**, 1846–1860.

Steinke S, Kienast M, Hanebuth T (2003) On the significance of sea-level variations and shelf paleo-morphology in governing sedimentation in the southern South China Sea during the last deglaciation. *Marine Geology*, **201**, 179–206.

Susilo GE, Yamamoto K, Imai T (2013) Modeling groundwater level fluctuation in the tropical peatland areas under the effect of El Niño. *Procedia Environmental Sciences*, **17**, 119–128.

Tuittila E-S, Juutinen S, Frolking S *et al*. (2012) Wetland chronosequence as a model of peatland development: vegetation succession, peat and carbon accumulation. *The Holocene*, **23**, 25–35.

Turetsky MR, Bond-Lamberty B, Euskirchen E, Talbot J, Frolking S, McGuire AD, Tuittila E-S (2012) The resilience and functional role of moss in boreal and arctic ecosystems. *The New phytologist*, **196**, 49–67.

Verry ES, Boelter DH, Päivänen J, Nichols DS, Malterer T, Gafni A. 2011. Physical properties of organic soils. In: *Peatland Biogeochemistry and Watershed Hydrology at the Marcell Experimental Forest* (eds Kolka RK, Sebestyen SD, Verry ES, Brooks KN), pp. 135–176, CRC Press, Boca Raton, FL.

Wang Y, Cheng H, Edwards RL *et al*. (2005) The Holocene Asian monsoon: links to solar changes and North Atlantic climate. *Science*, **308**, 854–857.

Warren MW, Kauffman JB, Murdiyarso D *et al*. (2012) A cost-efficient method to assess carbon stocks in tropical peat soil. *Biogeosciences*, **9**, 4477–4485.

Wösten J, Ismail A, van Wijk A (1997) Peat subsidence and its practical implications: a case study in Malaysia. *Geoderma*, **78**, 25–36.

Wösten H, Ritzema H, Rieley JO (2010) *Assessment of Risks and Vulnerabilities of Tropical Peatland Carbon Pools: Mitigation and Restoration Strategies. Technical Report 3EU CARBOPEAT Project, Carbon-Climate-Human Interactions in Tropical Peatlands: Vulnerabilities, Risks & Mitigation Measu*. University of Leicester, UK.

Wust RA, Bustin R (2004) Late Pleistocene and Holocene development of the interior peat-accumulating basin of tropical Tasek Bera, Peninsular Malaysia. *Palaeogeography, Palaeoclimatology, Palaeoecology*, **211**, 241–270.

Yu Z (2011) Holocene carbon flux histories of the world's peatlands: global carbon-cycle implications. *The Holocene*, **21**, 761–774.

Yu Z, Loisel J, Brosseau DP, Beilman DW, Hunt SJ (2010) Global peatland dynamics since the Last Glacial Maximum. *Geophysical Research Letters*, **37**, L13402.

Yule CM, Gomez LN (2008) Leaf litter decomposition in a tropical peat swamp forest in Peninsular Malaysia. *Wetlands Ecology and Management*, **17**, 231–241.

Supporting Information

Additional Supporting Information may be found in the online version of this article:

Data S1. Cluster analysis of 20th century rainfall in El Niño, normal, and La Niña classes.

Figure S1. The dendrogram of the two-way cluster analysis using the monthly rainfall data (thickness of horizontal black bars) classified as the El Niño years. Four clusters of years, separated by horizontal dashed lines, were extracted from this analysis (P1, P2, P3, and P4). The *X*-axis and *Y*-axis represent month and year, respectively, with the rainfall depth shown for each month.

Figure S2. Same as Figure S1 with the rainfall data from normal years. Clusters are P5–P8.

Figure S3. Same as Figure S1 with the rainfall data from La Niña years. Clusters are P9–P12.

Figure S4. Mean monthly precipitation of each group derived by the cluster analysis (see Figures S1–S3) for El Niño (top), normal (middle), and La Niña (bottom) conditions. Values in the legends represent the probability for every rainfall group within the broad El Niño, normal, and La Niña precipitation regimes.